Geophysical Research Letters

RESEARCH LETTER
10.1029/2020GL087720

Shear-Parallel Tropical Convective Systems: Importance of Cold Pools and Wind Shear

Leah D. Grant[1], Mitchell W. Moncrieff[2], Todd P. Lane[3,4], and Susan C. van den Heever[1]

[1]Department of Atmospheric Science, Colorado State University, Fort Collins, CO, USA, [2]National Center for Atmospheric Research, Boulder, CO, USA, [3]School of Earth Science, The University of Melbourne, Parkville, Victoria, Australia, [4]ARC Centre of Excellence for Climate Extremes, Parkville, Victoria, Australia

Key Points:
- Idealized simulations of tropical oceanic convective systems with varying wind profiles are analyzed
- When cold pools are weakened, convective systems are more often oriented shear-parallel, especially under strong wind shear regimes
- Shear-parallel versus perpendicular orientation impacts cloud-radiation interactions, gravity waves, and precipitable water patterns

Supporting Information:
- Supporting Information S1

Correspondence to:
L. D. Grant,
leah.grant@colostate.edu

Citation:
Grant, L. D., Moncrieff, M. W., Lane, T. P., & van den Heever, S. C. (2020). Shear-parallel tropical convective systems: Importance of cold pools and wind shear. *Geophysical Research Letters*, *47*, e2020GL087720. https://doi.org/10.1029/2020GL087720

Received 27 FEB 2020
Accepted 26 MAY 2020
Accepted article online 9 JUN 2020

Abstract The impact of cold pools on line-orientated convective systems is assessed using idealized simulations of tropical oceanic convection under weak, moderate, and strong wind shear regimes. Cold pools are weakened by suppressing evaporation in the shallow subcloud layer. Analysis of objectively identified convective systems reveals that the convection with weaker cold pools is more often oriented parallel, rather than perpendicular, to the wind shear. The cold pool-induced orientation changes are most pronounced in the strong shear environment. Interactions between convective orientation and the tropical atmosphere are assessed. Simulations with shear-parallel convection demonstrate more top-of-atmosphere upwelling longwave radiation and less reflected shortwave radiation due to changes in convective anvils, faster-propagating larger-scale gravity waves, narrower cross-shear moisture distributions, and differences in convective momentum fluxes. The results highlight critical interactions across convective scales, mesoscales, and climate scales, as well as avenues for parameterizing structural modes of mesoscale-organized convection in global models.

Plain Language Summary Over tropical oceans, individual thunderstorms often cluster together into a collection of thunderstorms. The way in which these thunderstorm clusters are organized is important for many aspects of weather and climate. For example, for line-organized thunderstorm clusters, whether the line is oriented parallel or perpendicular to the winds is important for how the thunderstorms alter the winds and how their anvils reflect solar radiation. In this study, we investigate the influence of cold pools, which are evaporatively cooled regions of air near the surface below thunderstorms, on the orientation of line-organized thunderstorm clusters using computer model simulations. We find that line-organized thunderstorm clusters are oriented parallel to the winds more often when the cold pools are weaker. We also show that cold pools have a larger impact on the orientation of the thunderstorm line when the upper level winds are stronger. Finally, we show how the cold pool-induced changes to line-organized thunderstorms affect the tropical climate, meaning these effects are important for climate models.

1. Introduction

Over tropical oceans, a variety of mesoscale-organized deep convection occurs every day. Tropical convection directly affects tropical waves (e.g., Mapes, 1993), the general circulation (Riehl & Malkus, 1958; Schumacher et al., 2004), and momentum transports (LeMone et al., 1984; Moncrieff, 1981). It is therefore essential to understand the physical mechanisms leading to different tropical convective structural modes if we are to better characterize the interactions between the convective scale, the mesoscale, and the climate scale and to represent these interactions within earth system models (Moncrieff, 2010). Some types of mesoscale-organized convection have been widely studied, such as line-organized convection oriented perpendicular to the vertical wind shear. However, shear-parallel convection remains understudied and poorly understood despite being widely observed. In this study, we examine mechanisms leading to shear-parallel convection and the larger-scale impacts on the tropical atmosphere.

The far-reaching effects of mesoscale-organized tropical convection result in complex upscale feedbacks to the large-scale atmospheric circulation and its interaction with the land and ocean. Mesoscale-organized convection must therefore be either explicitly represented or parameterized in climate models. However, the energy and momentum transport by mesoscale circulations that can exchange entire atmospheric layers has been neglected in traditional parameterizations. Dubbed "slantwise layer overturning," quasi-steady

circulations are driven by the mesoscale horizontal pressure gradients generated by the collective effect of cumulus ensembles in sheared environments. These mesoscale transports fundamentally differ from lateral turbulent mixing by transient small cumulus that are represented by contemporary convective parameterizations (see Moncrieff, 1981, 1992, 2010 for details). The impacts of parameterizing mesoscale-organized convection are only beginning to be explored in global climate models with encouraging progress (Ahn et al., 2019; Goswami et al., 2017; Moncrieff, 2019; Moncrieff et al., 2017).

Many significant advances in our understanding of mesoscale-organized tropical convection are attributable to comprehensive international field experiments, notably GATE (Houze & Betts, 1981) in the eastern Atlantic intertropical convergence zone (ITCZ) and TOGA COARE (Webster & Lukas, 1992) in the tropical western Pacific. Studies resulting from such campaigns documented a variety of convective organizational regimes (e.g., Alexander & Young, 1992; Johnson et al., 2005; LeMone et al., 1998). Deep convective bands parallel to the low- or mid-level shear have been commonly observed in GATE, TOGA COARE, and other field campaigns but have seldom been studied or numerically simulated compared to the shear-perpendicular systems. A few exceptions include simulated shear parallel convection under strong wind shear observed during GATE (Dudhia & Moncrieff, 1987) and numerical experiments of shear-parallel bands in the ITCZ (Khouider & Moncrieff, 2015). Most recently, Liu and Moncrieff (2017) investigated shear-parallel deep convection in simulations of an idealized mei-yu front in China. Their simulations included strong wind shear and a moisture tongue whose axis was parallel to the shear.

Recently, Guy and Jorgensen (2014) examined convective systems observed during the DYNAMO field campaign (Yoneyama et al., 2013) and found more numerous shear-parallel systems compared to TOGA COARE. They also used dropsonde observations and demonstrated that cold pools were weaker in DYNAMO than in TOGA COARE. These results help motivate our study. We ask the question: *do cold pools influence the orientation of line-organized systems*? Grant et al. (2018; hereafter GLv18) examined the role of cold pools in linear (shear-perpendicular) convective systems under weak wind shear conditions. They found that cold pools weakened the convective intensities because the negatively buoyant cold pool air was entrained into updrafts, similar to the findings of Liu and Moncrieff (2017) for the idealized mei-yu front system. GLv18 also showed that the cold pools were not the primary mechanism affecting the mesoscale organization of the convective systems. However, Guy and Jorgensen's results raise interesting questions about the role of cold pools in mesoscale-organized convection other than shear-perpendicular lines. In observations, strong shear at low- and mid-levels can lead to convective bands both parallel and perpendicular to the shear (Johnson et al., 2005; LeMone et al., 1998). Therefore, we also ask the question: *does the impact of cold pools on line-organized convective system orientation vary as a function of wind shear strength*?

We use idealized numerical simulations of convective systems in large-domain channel experiments with varying background wind shear strengths to address these questions. We investigate the influence of cold pools on the convective system properties and find that cold pools have substantial impacts on the convective orientation. We also find that the magnitude of the impact depends on the background wind shear. Finally, we show important implications of the cold pool-induced changes in convective system orientation on aspects of the tropical climate, thereby highlighting critical interactions across convective scales, mesoscales, and climate scales.

2. Methodology

2.1. Numerical Experiments

Large-domain, idealized numerical simulations of tropical oceanic convection are used to address the goals of this study. Idealized simulations provide a simple yet powerful framework within which to isolate and evaluate physical processes without confounding factors in more complex case-study simulations. The simulations are conducted with the Regional Atmospheric Modeling System (RAMS; Cotton et al., 2003) and are configured similar to many prior channel simulations of radiative-convective equilibrium (RCE). However, we only run the simulations part way to equilibrium, similar to McGee and van den Heever (2014) and GLv18. This transitional-RCE approach provides a number of advantages: (a) multiple convective systems exist simultaneously within the domain, allowing robust evaluations of responses in convective system properties to perturbations in the simulations; (b) the convective systems are not directly forced by the initial

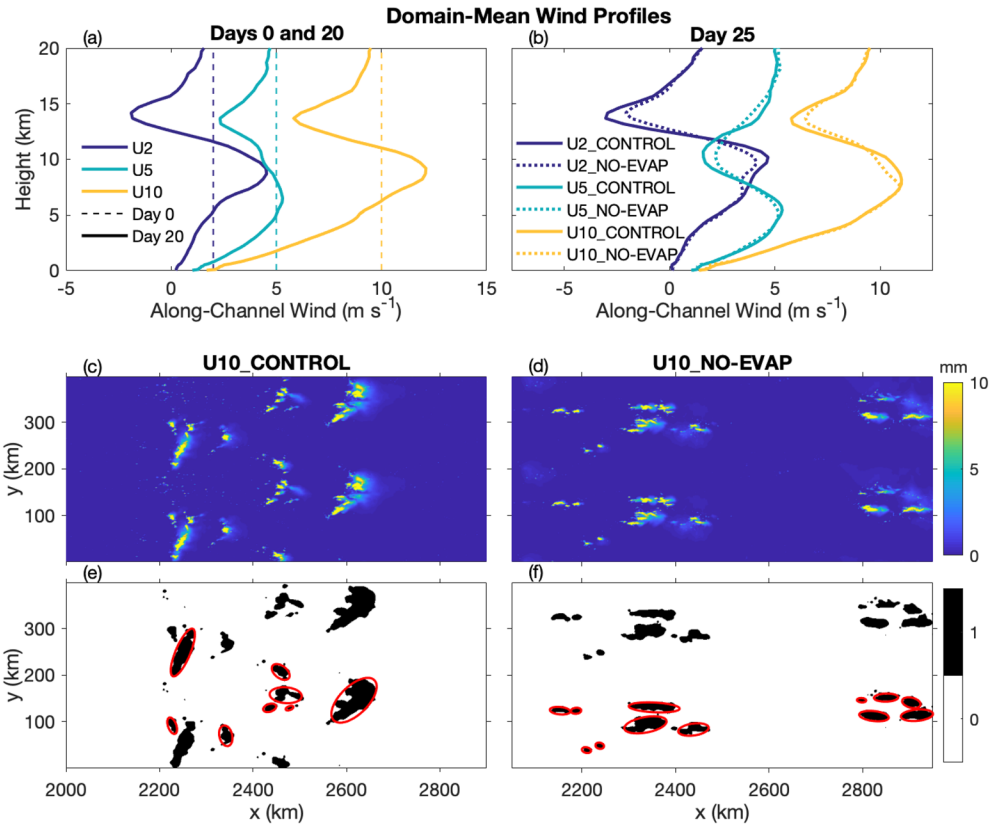

Figure 1. (a, b) Domain-mean along-channel wind speed (u) profiles at (a) Day 0 (dashed lines) and Day 20 (solid lines) for the CONTROL simulations and (b) Day 25 for all six simulations. (c–f) Plan views of (c, d) vertically integrated condensate (mm) and (e, f) corresponding connected regions. (c, e) U10_CONTROL at Day 24 hour 20; (d, f) U10_NO-EVAP at Day 24 hour 14. Fitted ellipses for unique identified convective features that meet the minimum area criteria (see Text S2) are plotted in red. Note that the y dimension is repeated twice, only a fraction of the x domain is shown, and axes aspect ratios are true-to-size.

conditions (e.g., warm bubbles); (c) the convective systems evolve in concert with their environment, resulting in a dynamically self-consistent framework; (d) the environment slowly evolves in time, analogous to real tropical environments subject to large-scale forcing such as from equatorial waves; and (e) the convective system properties in these transitional RCE states are realistic when compared to observed properties of tropical convective systems (e.g., GLv18). Points (b) and (c) are also true in RCE, but point (a) is not true in RCE if the domain size is too small or the final RCE state leads to only one or two large aggregated systems. Therefore, points (a), (d), and (e) are advantages to the transitional-RCE approach used here.

The setup of the simulations is fully described in supporting information Text S1 and closely follows the base simulation described in GLv18. Importantly, the domain size is 3,000 × 200 km^2 with 1 km horizontal grid spacing and 75 vertical levels. The SST is fixed at 300 K. A key difference in our experiment setup compared to GLv18 is the initial wind profile. While GLv18 initialized their simulation with no background wind, we initialize three separate simulations with different horizontally and vertically homogeneous along-channel (u) wind profiles (the cross-channel initial wind, v, is zero everywhere). Different initial wind speeds are used: 2, 5, and 10 m s^{-1} (Figure 1a), hereafter called U2_CONTROL, U5_CONTROL, and U10_CONTROL, respectively. We run each simulation for 25 days. Since the winds freely evolve throughout the simulations, the domain-mean wind profiles develop different amounts of shear through surface friction and convective momentum transport (Figure 1a). The U2_CONTROL simulation has the weakest (surface to 5 km AGL) shear, while U10_CONTROL has the strongest shear. The mean shear is predominantly in the x-direction.

We conduct three additional sensitivity experiments called U2_NO-EVAP, U5_NO-EVAP, and U10_NO-EVAP to assess the importance of cold pools to the convective system properties. In the NO-EVAP experiments, evaporation is suppressed in the subcloud layer using the same technique as GLv18. Each of these three NO-EVAP experiments is initialized from the corresponding CONTROL simulation at Day 20 and then run until Day 25. We suppress evaporation only below cloud base (400 m AGL) as an effective method to eliminate small cold pools and weaken large/intense cold pools. This has a minimal effect on gravity wave modes due to the shallowness of the evaporation change. Additionally, it does not directly alter processes such as cloud-edge evaporation and entrainment.

2.2. Analysis of Convective Properties

We use the MATLAB image processing toolbox to robustly assess differences in convective system properties when the cold pools are altered. We objectively identify convective objects, fit ellipses to the identified systems (Figures 1c–1f), and collect statistics such as aspect ratio (i.e., linearity) and angle from the shear vector. Full details are provided in Text S2. Linear systems are defined as those whose fitted ellipses have aspect ratios of 2:5 or smaller (Xu & Rutledge, 2015). A similar ellipse-fitting approach has been previously used for object-based analysis of convective systems in TRMM satellite observations, radar scans, and simulations (Caine et al., 2013; Liu & Zipser, 2013; Nesbitt et al., 2006; Xu & Rutledge, 2015).

3. System Orientation

The convective system snapshots in Figures 1c–1f demonstrate a stark difference in orientation between the U10_CONTROL and U10_NO-EVAP simulations. Recall that the shear vector points in the positive x-direction: In U10_CONTROL, although the convective systems are oriented at an angle to the shear vector, their orientation is closer to shear-perpendicular than shear-parallel. However, the convective system orientations in U10_NO-EVAP are shear-parallel, suggesting that cold pools affect the convective system orientation.

Figures 2a and 2b summarize the linearity and orientation of the large (area $\geq$ 500 km^2) convective objects identified in U10_CONTROL and U10_NO-EVAP (the results are similar for the entire convective object database; see Figure S1). The convection with weaker cold pools (U10_NO-EVAP) is oriented in the shear-parallel direction more frequently than the convection with stronger cold pools (U10_CONTROL), regardless of the linearity.

We next examine the differences between the linear system orientations from Days 22–25 for all six simulations (see Figure S1 for the temporal evolution of the convective orientation). The results (Figure 2c) demonstrate that the U10 simulation behavior also holds for the other simulation pairs: The convective objects with weaker cold pools (NO-EVAP) are oriented in the shear-parallel direction more often than the objects with stronger cold pools (CONTROL). However, the details of this response depend on the background wind shear. The variability in convective orientation is more noticeably reduced in the NO-EVAP simulations under the strongest wind shear environment, particularly in the interquartile range of the data (Figure 2c). Specifically, the interquartile range decreases from 28.9° in U2_CONTROL to 21.4° in U2_NO-EVAP or by 26%; by 37% (23.5° to 14.9°) for the U5 simulations; and by 51% (18.2° to 9.0°) in the U10 cases. This indicates that the cold pools are more influential in determining the convective system orientation under the stronger background wind shear regime than the weaker wind shear scenario. This result is in keeping with GLv18 because the wind shear in those simulations was even weaker than the U2 simulations examined here, although GLv18 did not examine orientation changes nor were their simulations run for longer than 1.5 days.

Why then do the convective systems become shear-parallel more often in the weak cold pools simulations? And why is the variability in orientation more strongly reduced under the larger shear scenarios? Our hypothesis is in the CONTROL simulations, the cold pools are strong enough to spread out laterally in the shear-perpendicular direction. This exposes more distance along the downshear side of cold pool edge to the perpendicular wind flow, which is known to be the most favorable portion of the cold pool to initiate new convection (e.g., Moncrieff & Liu, 1999; Rotunno et al., 1988; Thorpe et al., 1982). These initiation patterns would lead to shear-perpendicular systems or to arced convective systems when we consider a temporal lag between the cold pool cross-shear propagation and the subsequent convective initiation.

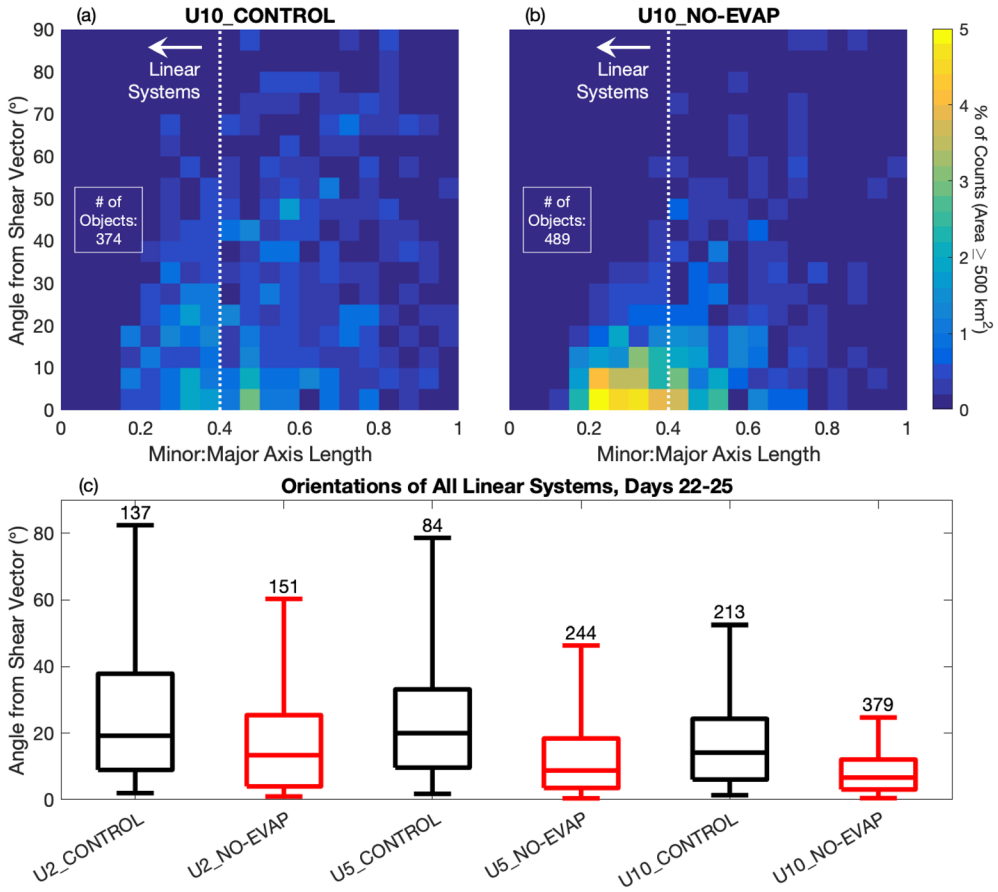

Figure 2. (a, b) 2-D histograms showing the frequency of different linearity and orientation angle combinations for convective objects with area ≥ 500 km^2 in (a) U10_CONTROL and (b) U10_NO-EVAP. The dotted line separates linear and not-linear systems. (c) Box plots comparing the orientations of all linear systems among all simulations for Days 22–25. Box and whisker values represent 5th, 25th, 50th, 75th, and 95th percentiles. The number of features in each box plot is listed above the upper whisker.

Arced systems are evident in Figure 1c, as well as in Robe and Emanuel (2001). On the other hand, when the cold pools are weakened or eliminated in the NO-EVAP simulations, the cold pools do not propagate laterally in the cross-shear direction. The largest decrease in cold pool cross-shear propagation occurs in the U10 simulations (see Figure S2 for support of this statement). Our explanation agrees with Emanuel (1986) and Robe and Emanuel (2001): They found that squall-lines rotate away from the shear-perpendicular direction as the magnitude of the shear overwhelms the cold pool. Here, we see this effect by changing the cold pools, rather than by changing the shear. It is also possible that shallow gravity wave modes (e.g., Tulich & Mapes, 2008) become important convective initiation mechanisms in the down- or up-shear direction (e.g., Lane & Moncrieff, 2015; Liu & Moncrieff, 2017) when the cold pools are removed.

The following section describes implications of these results for mesoscales and climate scales including cloud-radiation interactions and hence climate-relevant impacts, convectively-generated gravity waves, and precipitable water.

4. Broader Implications

4.1. Cloud-Radiation Interactions

The domain-mean outgoing longwave radiation (OLR) at the top of the atmosphere (TOA) increases in all three NO-EVAP simulations relative to the CONTROL simulations, by up to 3.5 W m^{-2} (Table S1). The

domain-mean TOA upwelling reflected shortwave radiation (SWup) decreases by up to 4.7 W m^{-2} (Table S1). Overall, the changes in outgoing shortwave and longwave radiation between the CONTROL and NO-EVAP simulations have opposite sign. While this means that the net radiative change at TOA is small, the change in shortwave versus longwave partitioning has implications for column-heating rates and feedbacks to sea surface temperature.

To examine the mechanisms for the changes in radiative flux partitioning, we only discuss the U10 simulations for simplicity. The increase in OLR and decrease in TOA SWup in U10_NO-EVAP are primarily due to an increase in the number of cloud-free columns (defined as columns where total condensate is everywhere less than 0.01 g kg^{-1}). The frequency of cloud-free columns through Days 22–25 increases from 51% in U10_CONTROL to 54% in U10_NO-EVAP. This means that (i) more OLR escapes through the TOA on average because more longwave radiation is emitted from the lower, warmer regions of the atmosphere, and (ii) less shortwave radiation is reflected on average because the ocean surface is darker than the clouds. The change in cloud-free column frequency can be explained by the convective orientation changes. Shear-parallel systems have narrower anvils than shear-perpendicular systems because the convection that feeds the anvils forms parallel to the axis of upper level winds that advect the anvil downstream. This effect was hypothesized in Johnson et al. (2005). Given the critical role of cloud-radiative forcing in climate processes (e.g., Hartmann & Short, 1980; Ramanathan et al., 1989), these demonstrated radiative results suggest that the mesoscale orientation of convective systems is important for climate scales, thus highlighting the importance of understanding environmental conditions and physics governing shear-parallel convective systems and their associated anvils.

4.2. Convectively-Generated Gravity Waves

The simulated convective systems initiate, propagate, and dissipate through the influence of larger-scale gravity waves (Figures 3a, 3b, 3d, 3e, 3g, and 3h), resembling numerous other studies (e.g., GLv18; Lane & Moncrieff, 2008; Lane & Zhang, 2011; Tulich & Mapes, 2008). The gravity waves are evident by the pressure contours and the co-located dots marking the locations of the maximum surface pressure perturbation and minimum low-level potential temperature perturbation (θ'), as expected from the combined gravity wave response to convective and stratiform heating (e.g., Nicholls et al., 1991). Figure 3 demonstrates that the gravity waves propagate faster in the NO-EVAP simulations than in the CONTROL simulations. The faster speeds are deduced by comparing the positions of the pressure and temperature signals between each pair of simulations. We quantify the change in gravity wave propagation speed in the U5 simulations as described in Text S3. The resulting gravity wave propagation speed is 17.0 m s^{-1} in U5_CONTROL and 18.7 m s^{-1} in U5_NO-EVAP, representing a 10% increase in U5_NO-EVAP.

The faster gravity wave propagation speeds in the NO-EVAP simulations can be explained by the vertical profiles of θ'. The altitude of the low-level θ' minimum increases in the NO-EVAP cases by 0.2–0.45 km or 7–15% (Figures 3c, 3f, and 3i). This altitude change in the lowermost antinode implies a slight increase in the vertical wavelength, which can help explain the magnitude of the speed change because hydrostatic gravity wave propagation speed is directly proportional to the vertical wavelength. The longer vertical wavelengths in the NO-EVAP simulations are likely related to the lack of near-surface cooling and thus to the weaker cold pools compared to the CONTROL cases. Additionally, longer vertical wavelengths in the U2 and U5 NO-EVAP cases can also be explained by increases in the uppermost node depth. These increases are related to deeper convection in U2_NO-EVAP and more frequent deep convection in U5_NO-EVAP (see Figures S3a and S3b, which shows PDFs of maximum cloud top heights). Thus, the convective system orientation has implications for convectively coupled wave propagation speeds and spatio-temporal patterns of convective activity and lifetimes.

4.3. Water-Vapor Distribution

We also examine the effects of convective system orientation on the thermodynamic environment, specifically, the spatio-temporal patterns of precipitable water (PW). It is known that convection in the tropics is sensitive to environmental moisture (e.g., Brown & Zhang, 1997; Derbyshire et al., 2004; Kumar et al., 2015). We ask whether the changes in the convective behavior impact the PW? To address this question, we examine the cross-shear moisture distribution by standardizing, centering, and sorting the PW field and averaging over the moistest quartile (see Text S4 for details and Figure S4 for an illustrated example). The result,

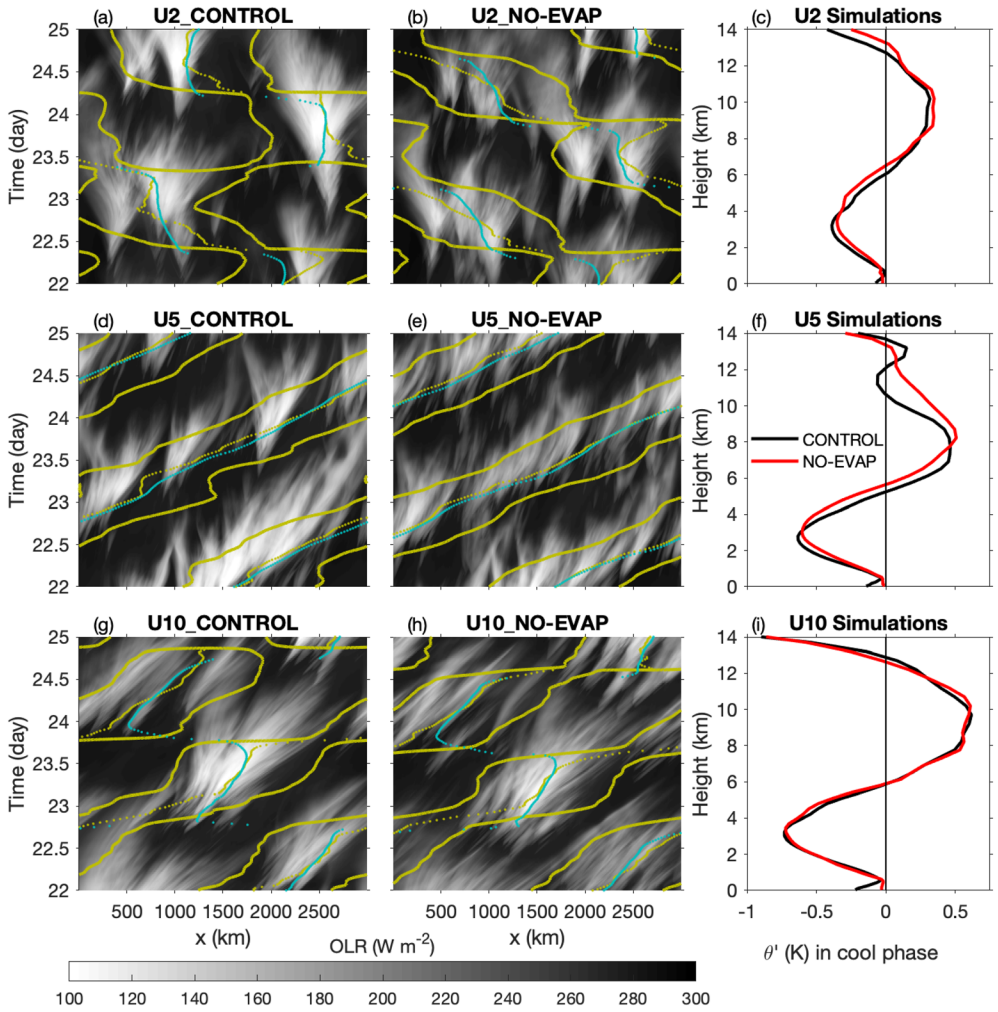

Figure 3. (a, b, d, e, g, h) Hovmöller diagrams of y-averaged quantities: OLR (shaded); smoothed surface pressure perturbation (+0.02 hPa, gold contours); and locations of the maxima in smoothed surface pressure perturbation (gold dots) and minima in smoothed 3 km AGL potential temperature perturbation θ'_{3km} (blue dots) at each time. Pressure and θ'_{3km} fields were smoothed using a triangular filter with a span of 2,000 km. Only Days 22–25 are shown. (c, f, i) Profiles of θ' in the low-level cool phase of the larger-scale wave (i.e., where smoothed $\theta'_{3km} < 0$), averaged over Days 22–25. All perturbations are relative to the domain-mean.

displayed in Figure 4, shows that the PW distribution is narrower in the cross-shear direction in the NO-EVAP simulations, particularly after Day 22. This result follows from the changes in near-surface v wind distributions (Figure S2), which transport water vapor in the cross-shear direction. Thus, the convective system orientation affects the tropical thermodynamic environment.

4.4. Convective Momentum Transport

Momentum fluxes in shear-parallel convection are down-gradient, whereas the momentum fluxes in shear-perpendicular convection can be either up- or down-gradient depending on the system tilt (LeMone et al., 1984; Moncrieff, 1981, 1997). Therefore, we expect changes in the convective orientation to lead to different momentum fluxes and feedbacks to the mean wind profile. Figure 1b demonstrates that the mean wind profile is smoother above 5 km AGL in the NO-EVAP experiments compared to the CONTROL simulations. This response is expected: The NO-EVAP simulations have more frequent shear-parallel convection, momentum fluxes in shear-parallel convection are down-gradient, and down-gradient momentum fluxes act to decrease shear.

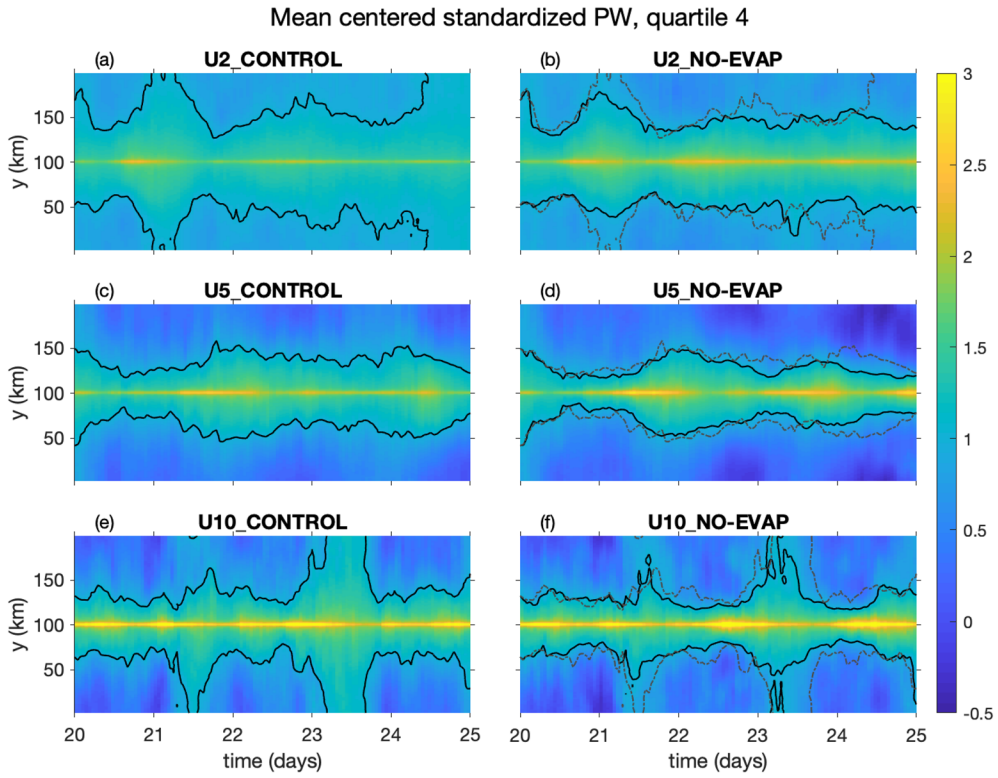

Figure 4. Hovmöller diagrams showing the *y*-distribution of the centered, standardized PW averaged over the moistest quartile (shading); see Text S4 for details. Black contours indicate +1 standardized PW for each simulation. For comparison purposes, the gray dash-dot contours in (b), (d), and (f) show the +1 standardized PW from the corresponding CONTROL simulation.

5. Conclusions

The physics of shear-parallel convection remain understudied and poorly understood, yet critical for understanding the tropical atmosphere as demonstrated herein. We examined the impact of changes in cold pool properties on tropical oceanic convective system orientations under different wind shear regimes using idealized channel simulations of tropical oceanic convection. We showed that linear convective systems are more often shear-parallel oriented in simulations with weaker cold pools compared to simulations with stronger cold pools. The orientation changes are more pronounced in a strong wind shear environment than in weak shear. These results point to an important role of cold pools in tropical convective system morphology related to the propensity for cold pools to propagate in the cross-shear direction and initiate convection on the downshear side of the cold pool. Additional analyses examining the detailed dynamical flow regimes and behavior of shear-parallel convective systems are the subject of a follow-up study.

We also examined the links between the convective scale, mesoscale, and climate scale by assessing the interactions between the convective orientation and the tropical environment. The simulations with more frequent shear-parallel convection have more top-of-atmosphere upwelling longwave radiation and less reflected shortwave radiation due to narrower anvils. These same simulations also have faster-propagating larger-scale gravity waves due to differences in the heating profiles and narrower moisture tongues in the cross-shear direction. The moisture results are analogous to the idealized shear-parallel mei-yu front convection (Liu & Moncrieff, 2017) since the shear, convection, and moisture axes were all oriented in the same direction. Finally, the mean wind profile in the simulations with more frequent shear-parallel convection is smoother due to differences in the convective momentum fluxes. The interactions between shear-parallel convection and the tropical environment suggest new avenues for parameterization development and evaluation in climate models. This is particularly salient to the ITCZ and Indian Ocean, where shear-parallel mesoscale organization is widely observed (e.g., GATE and DYNAMO). It follows that the

parameterization of momentum transport in the ITCZ locale should be down-gradient (Khouider & Moncrieff, 2015; Moncrieff, 1997).

Overall, moist tropical environments where cold pools are weak and propagate slowly may be conducive to shear-parallel systems, as shown by our idealized simulations and observed in field campaigns. Our results are consistent with the DYNAMO observations of more frequent shear-parallel convection and weaker cold pools than TOGA COARE squall lines (Guy & Jorgensen, 2014). Finally, the feedbacks between convective orientation and precipitable water structure could have implications for RCE studies. Our cross-shear moisture distribution results may explain why RCE channel simulations exhibit band-like structures, rather than "clumps" in square-domain simulations. These topics are avenues for further investigation.

Acknowledgments
We thank two anonymous reviewers whose comments improved the manuscript clarity and content. This work was supported by NASA grant NNX16AO93G, Office of Naval Research grant N000141613093, and the Australian Research Council's Centres of Excellence Scheme (CE170100023). Data Availability Statement: Source code used in this study is available for download from the CSU Mountain Scholar digital repository (https://hdl.handle.net/10217/205802) (Grant et al., 2020).

References

Ahn, M., Kim, D., Park, S., & Ham, Y. (2019). Do we need to parameterize mesoscale convective organization to mitigate the MJO-mean state trade-off? *Geophysical Research Letters*, *46*, 2293–2301. https://doi.org/10.1029/2018GL080314

Alexander, G. D., & Young, G. S. (1992). The relationship between EMEX mesoscale precipitation feature properties and their environmental characteristics. *Monthly Weather Review*, *120*(4), 554–564. https://doi.org/10.1175/1520-0493(1992)120<0554:TRBEMP>2.0.CO;2

Brown, R. G., & Zhang, C. (1997). Variability of midtropospheric moisture and its effect on cloud-top height distribution during TOGA COARE*. *Journal of the Atmospheric Sciences*, *54*(23), 2760–2774. https://doi.org/10.1175/JAS3614.1

Caine, S., Lane, T. P., May, P. T., Jakob, C., Siems, S. T., Manton, M. J., & Pinto, J. (2013). Statistical assessment of tropical convection-permitting model simulations using a cell-tracking algorithm. *Monthly Weather Review*, *141*(2), 557–581. https://doi.org/10.1175/MWR-D-11-00274.1

Cotton, W. R., Pielke Sr, R. A., Walko, R. L., Liston, G. E., Tremback, C. J., Jiang, H., et al. (2003). RAMS 2001: Current status and future directions. *Meteorology and Atmospheric Physics*, *82*(1–4), 5–29. https://doi.org/10.1007/s00703-001-0584-9

Derbyshire, S. H., Beau, I., Bechtold, P., Grandpeix, J.-Y., Piriou, J.-M., Redelsperger, J.-L., & Soares, P. M. M. (2004). Sensitivity of moist convection to environmental humidity. *Quarterly Journal of the Royal Meteorological Society*, *130*(604), 3055–3079. https://doi.org/10.1256/qj.03.130

Dudhia, J., & Moncrieff, M. W. (1987). A numerical simulation of quasi-stationary tropical convective bands. *Quarterly Journal of the Royal Meteorological Society*, *113*(477), 929–967. https://doi.org/10.1002/qj.49711347711

Emanuel, K. A. (1986). Some dynamical aspects of precipitating convection. *Journal of the Atmospheric Sciences*, *43*(20), 2183–2198. https://doi.org/10.1175/1520-0469(1986)043<2183:SDAOPC>2.0.CO;2

Goswami, B. B., Khouider, B., Phani, R., Mukhopadhyay, P., & Majda, A. J. (2017). Improved tropical modes of variability in the NCEP climate forecast system (version 2) via a stochastic multicloud model. *Journal of the Atmospheric Sciences*, *74*(10), 3339–3366. https://doi.org/10.1175/JAS-D-17-0113.1

Grant, L. D., Lane, T. P., & van den Heever, S. C. (2018). The role of cold pools in tropical oceanic convective systems. *Journal of the Atmospheric Sciences*, *75*(8), 2615–2634. https://doi.org/10.1175/JAS-D-17-0352.1

Grant, L. D., Moncrieff, M. W., Lane, T. P., & van den Heever, S. C. (2020). Source code associated with "Shear-Parallel Tropical Convective Systems: Importance of Cold Pools and Wind Shear." Colorado State University. Libraries. https://doi.org/10.25675/10217/205802

Guy, N., & Jorgensen, D. P. (2014). Kinematic and precipitation characteristics of convective systems observed by airborne Doppler radar during the life cycle of a Madden–Julian oscillation in the Indian Ocean. *Monthly Weather Review*, *142*(4), 1385–1402. https://doi.org/10.1175/MWR-D-13-00252.1

Hartmann, D. L., & Short, D. A. (1980). On the use of earth radiation budget statistics for studies of clouds and climate. *Journal of the Atmospheric Sciences*, *37*(6), 1233–1250. https://doi.org/10.1175/1520-0469(1980)037<1233:OTUOER>2.0.CO;2

Houze, R. A., & Betts, A. K. (1981). Convection in GATE. *Reviews of Geophysics*, *19*(4), 541–576. https://doi.org/10.1029/RG019i004p00541

Johnson, R. H., Aves, S. L., Ciesielski, P. E., & Keenan, T. D. (2005). Organization of oceanic convection during the onset of the 1998 east Asian summer monsoon. *Monthly Weather Review*, *133*(1), 131–148. https://doi.org/10.1175/MWR-2843.1

Khouider, B., & Moncrieff, M. W. (2015). Organized convection parameterization for the ITCZ. *Journal of the Atmospheric Sciences*, *72*(8), 3073–3096. https://doi.org/10.1175/JAS-D-15-0006.1

Kumar, V. V., Jakob, C., Protat, A., Williams, C. R., & May, P. T. (2015). Mass-flux characteristics of tropical cumulus clouds from wind profiler observations at Darwin, Australia. *Journal of the Atmospheric Sciences*, *72*(5), 1837–1855. https://doi.org/10.1175/JAS-D-14-0259.1

Lane, T. P., & Moncrieff, M. W. (2008). Stratospheric gravity waves generated by multiscale tropical convection. *Journal of the Atmospheric Sciences*, *65*(8), 2598–2614. https://doi.org/10.1175/2007JAS2601.1

Lane, T. P., & Moncrieff, M. W. (2015). Long-lived mesoscale systems in a low–convective inhibition environment. Part I: Upshear propagation. *Journal of the Atmospheric Sciences*, *72*(11), 4297–4318. https://doi.org/10.1175/JAS-D-15-0073.1

Lane, T. P., & Zhang, F. (2011). Coupling between gravity waves and tropical convection at mesoscales. *Journal of the Atmospheric Sciences*, *68*(11), 2582–2598. https://doi.org/10.1175/2011JAS3577.1

LeMone, M. A., Barnes, G. M., & Zipser, E. J. (1984). Momentum flux by lines of cumulonimbus over the tropical oceans. *Journal of the Atmospheric Sciences*, *41*(12), 1914–1932. https://doi.org/10.1175/1520-0469(1984)041<1914:MFBLOC>2.0.CO;2

LeMone, M. A., Zipser, E. J., & Trier, S. B. (1998). The role of environmental shear and thermodynamic conditions in determining the structure and evolution of mesoscale convective systems during TOGA COARE. *Journal of the Atmospheric Sciences*, *55*(23), 3493–3518. https://doi.org/10.1175/1520-0469(1998)055<3493:TROESA>2.0.CO;2

Liu, C., & Moncrieff, M. W. (2017). Shear-parallel mesoscale convective systems in a moist low-inhibition mei-yu front environment. *Journal of the Atmospheric Sciences*, *74*(12), 4213–4228. https://doi.org/10.1175/JAS-D-17-0121.1

Liu, C., & Zipser, E. (2013). Regional variation of morphology of organized convection in the tropics and subtropics. *Journal of Geophysical Research: Atmospheres*, *118*, 453–466. https://doi.org/10.1029/2012JD018409

Mapes, B. E. (1993). Gregarious tropical convection. *Journal of the Atmospheric Sciences*, *50*(13), 2026–2037. https://doi.org/10.1175/1520-0469(1993)050%3C2026:GTC%3E2.0.CO;2

McGee, C. J., & van den Heever, S. C. (2014). Latent heating and mixing due to entrainment in tropical deep convection. *Journal of the Atmospheric Sciences*, *71*(2), 816–832. https://doi.org/10.1175/JAS-D-13-0140.1

Moncrieff, M. W. (1981). A theory of organized steady convection and its transport properties. *Quarterly Journal of the Royal Meteorological Society*, *107*(451), 29–50. https://doi.org/10.1256/smsqj.45102

Moncrieff, M. W. (1992). Organized convective systems: Archetypal dynamical models, mass and momentum flux theory, and parametrization. *Quarterly Journal of the Royal Meteorological Society*, *118*(507), 819–850. https://doi.org/10.1002/qj.49711850703

Moncrieff, M. W. (1997). Momentum transport by organized convection. In R. K. Smith (Ed.), *The Physics and Parameterization of Moist Atmospheric Convection NATO ASI Series, Series C: Mathematical and Physical Sciences*, (Vol. 505, pp. 231–253). Dordrecht, Netherlands: Springer. https://doi.org/10.1007/978-94-015-8828-7_9

Moncrieff, M. W. (2010). The multiscale organization of moist convection and the intersection of weather and climate. In D.-Z. Sun, & F. Bryan (Eds.), *Climate Dynamics: Why Does Climate Vary? Geophysical Monograph Series*, (Vol. 189, pp. 3–26). Washington, DC: American Geophysical Union. https://doi.org/10.1029/2008GM000838

Moncrieff, M. W. (2019). Toward a dynamical foundation for organized convection parameterization in GCMs. *Geophysical Research Letters*, *46*, 14,103–14,108. https://doi.org/10.1029/2019GL085316

Moncrieff, M. W., & Liu, C. (1999). Convection initiation by density currents: Role of convergence, shear, and dynamical organization. *Monthly Weather Review*, *127*(10), 2455–2464. https://doi.org/10.1175/1520-0493(1999)127<2455:CIBDCR>2.0.CO;2

Moncrieff, M. W., Liu, C., & Bogenschutz, P. (2017). Simulation, modeling, and dynamically based parameterization of organized tropical convection for global climate models. *Journal of the Atmospheric Sciences*, *74*(5), 1363–1380. https://doi.org/10.1175/JAS-D-16-0166.1

Nesbitt, S. W., Cifelli, R., & Rutledge, S. A. (2006). Storm morphology and rainfall characteristics of TRMM precipitation features. *Monthly Weather Review*, *134*(10), 2702–2721. https://doi.org/10.1175/MWR3200.1

Nicholls, M. E., Pielke, R. A., & Cotton, W. R. (1991). Thermally forced gravity waves in an atmosphere at rest. *Journal of the Atmospheric Sciences*, *48*(16), 1869–1884. https://doi.org/10.1175/1520-0469(1991)048<1869:TFGWIA>2.0.CO;2

Ramanathan, V., Cess, R. D., Harrison, E. F., Minnis, P., Barkstrom, B. R., Ahmad, E., & Hartmann, D. (1989). Cloud-radiative forcing and climate: Results from the Earth Radiation Budget Experiment. *Science*, *243*(4887), 57–63. https://doi.org/10.1126/science.243.4887.57

Riehl, H., & Malkus, J. S. (1958). On the heat balance in the equatorial trough zone. *Geophysica*, *6*(3–4), 503–538.

Robe, F. R., & Emanuel, K. A. (2001). The effect of vertical wind shear on radiative–convective equilibrium states. *Journal of the Atmospheric Sciences*, *58*(11), 1427–1445. https://doi.org/10.1175/1520-0469(2001)058<1427:TEOVWS>2.0.CO;2

Rotunno, R., Klemp, J. B., & Weisman, M. L. (1988). A theory for strong, long-lived squall lines. *Journal of the Atmospheric Sciences*, *45*(3), 463–485. https://doi.org/10.1175/1520-0469(1988)045<0463:ATFSLL>2.0.CO;2

Schumacher, C., Houze, R. A., & Kraucunas, I. (2004). The tropical dynamical response to latent heating estimates derived from the TRMM precipitation radar. *Journal of the Atmospheric Sciences*, *61*(12), 1341–1358. https://doi.org/10.1175/1520-0469(2004)061%3C1341:TTDRTL%3E2.0.CO;2

Thorpe, A. J., Miller, M. J., & Moncrieff, M. W. (1982). Two-dimensional convection in non-constant shear: A model of mid-latitude squall lines. *Quarterly Journal of the Royal Meteorological Society*, *108*(458), 739–762. https://doi.org/10.1002/qj.49710845802

Tulich, S. N., & Mapes, B. E. (2008). Multiscale convective wave disturbances in the tropics: Insights from a two-dimensional cloud-resolving model. *Journal of the Atmospheric Sciences*, *65*(1), 140–155. https://doi.org/10.1175/2007JAS2353.1

Webster, P. J., & Lukas, R. (1992). TOGA COARE: The coupled ocean-atmosphere response experiment. *Bulletin of the American Meteorological Society*, *73*(9), 1377–1416. https://doi.org/10.1175/1520-0477(1992)073<1377:TCTCOR>2.0.CO;2

Xu, W., & Rutledge, S. A. (2015). Morphology, intensity, and rainfall production of MJO convection: Observations from DYNAMO shipborne radar and TRMM. *Journal of the Atmospheric Sciences*, *72*(2), 623–640. https://doi.org/10.1175/JAS-D-14-0130.1

Yoneyama, K., Zhang, C., & Long, C. N. (2013). Tracking pulses of the Madden–Julian oscillation. *Bulletin of the American Meteorological Society*, *94*(12), 1871–1891. https://doi.org/10.1175/BAMS-D-12-00157.1

References From the Supporting Information

Bretherton, C. S., Blossey, P. N., & Khairoutdinov, M. (2005). An energy-balance analysis of deep convective self-aggregation above uniform SST. *Journal of the Atmospheric Sciences*, *62*(12), 4273–4292. https://doi.org/10.1175/JAS3614.1

Harrington, J. Y. (1997). The effects of radiative and microphysical processes on simulated warm and transition season Arctic stratus (Doctoral dissertation). Fort Collins, CO: Colorado State University. Retrieved from http://www.meteo.psu.edu/~jyh10/pubs/dis.pdf

Louis, J.-F. (1979). A parametric model of vertical eddy fluxes in the atmosphere. *Boundary-Layer Meteorology*, *17*(2), 187–202. https://doi.org/10.1007/BF00117978

Meyers, M. P., Walko, R. L., Harrington, J. Y., & Cotton, W. R. (1997). New RAMS cloud microphysics parameterization. Part II: The two-moment scheme. *Atmospheric Research*, *45*(1), 3–39. https://doi.org/10.1016/S0169-8095(97)00018-5

Saleeby, S. M., & Cotton, W. R. (2004). A large-droplet mode and prognostic number concentration of cloud droplets in the Colorado State University Regional Atmospheric Modeling System (RAMS). Part I: Module descriptions and supercell test simulations. *Journal of Applied Meteorology*, *43*(1), 182–195. https://doi.org/10.1175/1520-0450(2004)043<0182:ALMAPN>2.0.CO;2

Saleeby, S. M., & Cotton, W. R. (2008). A binned approach to cloud-droplet riming implemented in a bulk microphysics model. *Journal of Applied Meteorology and Climatology*, *47*(2), 694–703. https://doi.org/10.1175/2007JAMC1664.1

Saleeby, S. M., & van den Heever, S. C. (2013). Developments in the CSU-RAMS aerosol model: Emissions, nucleation, regeneration, deposition, and radiation. *Journal of Applied Meteorology and Climatology*, *52*(12), 2601–2622. https://doi.org/10.1175/JAMC-D-12-0312.1